

Fulde-Ferrell-Larkin-Ovchinnikov states in equally populated Fermi gases in a two-dimensional moving optical lattice

Jin-Ge Chen(陈金鸽), Yue-Ran Shi(石悦然), Ren Zhang(张仁), Kui-Yi Gao(高奎意), and Wei Zhang(张威)
Citation: Chin. Phys. B, 2021, 30 (**10**): 100305. DOI: 10.1088/1674-1056/abf346
Journal homepage: http://cpb.iphy.ac.cn; http://iopscience.iop.org/cpb

What follows is a list of articles you may be interested in

Fulde-Ferrell-Larkin-Ovchinnikov states in equally populated Fermi gases in a two-dimensional moving optical lattice

Jin-Ge Chen(陈金鸽), Yue-Ran Shi(石悦然), Ren Zhang(张仁), Kui-Yi Gao(高奎意), and Wei Zhang(张威)
Chin. Phys. B, 2021, 30 (**10**): 100305. DOI: 10.1088/1674-1056/abf346

Dynamical stability of dipolar condensate in a parametrically modulated one-dimensional optical lattice

Ji-Li Ma(马吉利), Xiao-Xun Li(李晓旬), Rui-Jin Cheng(程瑞锦), Ai-Xia Zhang(张爱霞), and Ju-Kui Xue(薛具奎)
Chin. Phys. B, 2021, 30 (**6**): 060307. DOI: 10.1088/1674-1056/abd746

Peierls-phase-induced topological semimetals in an optical lattice: Moving of Dirac points, anisotropy of Dirac cones, and hidden symmetry protection

Jing-Min Hou(侯净敏)
Chin. Phys. B, 2020, 29 (**12**): 120305. DOI: 10.1088/1674-1056/abc0de

Zitterbewegung of Dirac quasiparticles emerged in a Su-Schrieffer–Heeger lattice

Yue Hu(胡玥), Zheng-Xin Guo(郭政鑫), Ze-Ming Zhong(钟泽明), and Zhi Li(李志)
Chin. Phys. B, 2020, 29 (**11**): 110302. DOI: 10.1088/1674-1056/abb45b

Cyclotron dynamics of neutral atoms in optical lattices with additional magnetic field and harmonic trap potential

Ai-Xia Zhang(张爱霞), Ying Zhang(张莹), Yan-Fang Jiang(姜艳芳), Zi-Fa Yu(鱼自发), Li-Xia Cai(蔡丽霞), Ju-Kui Xue(薛具奎)
Chin. Phys. B, 2020, 29 (**1**): 010307. DOI: 10.1088/1674-1056/ab5efc

---

Fulde–Ferrell–Larkin–Ovchinnikov states in equally populated Fermi gases in a two-dimensional moving optical lattice*

Jin-Ge Chen(陈金鸽)[1], Yue-Ran Shi(石悦然)[1], Ren Zhang(张仁)[2], Kui-Yi Gao(高奎意)[1,3,†], and Wei Zhang(张威)[1,3,‡]

[1] *Department of Physics, Renmin University of China, Beijing* 100872, *China*
[2] *School of Physics, Xi'an Jiaotong University, Xi'an* 710049, *China*
[3] *Beijing Key Laboratory of Opto-electronic Functional Materials and Micro-nano Devices, Renmin University of China, Beijing* 100872, *China*

(Received 3 March 2021; revised manuscript received 23 March 2021; accepted manuscript online 30 March 2021)

We study the possibility of stabilizing a Fulde–Ferrell–Larkin–Ovchinnikov (FFLO) state in an equally populated two-component Fermi gas trapped in a moving two-dimensional optical lattice. For a system with nearly half filling, we find that a finite pairing momentum perpendicular to the moving direction can be spontaneously induced for a proper choice of lattice velocity. As a result, the total pairing momentum is tilted towards the nesting vector to take advantage of the significant enhancement of the density of states.

Keywords: FFLO state, optical lattice, ultracold Fermi gas, superfluid

PACS: 03.75.Ss, 03.75.Hh, 05.30.Fk **DOI:** 10.1088/1674-1056/abf346

1. Introduction

After its first proposal in 1960s, the search for the unconventional pairing Fulde–Ferrell–Larkin–Ovchinnikov (FFLO) states[1,2] persists for more than half a century. The original idea of the previously studied FFLO state is to look for a compromised candidate for superconducting states which can sustain a finite magnetization. This exotic pairing state is characterized by a superconducting order parameter with one or more nonzero components of a finite momentum $\boldsymbol{q}$, hence breaks both translational and rotational symmetry and forms a crystal of pairing order. In the past several decades, the existence of FFLO states was studied in various systems,[3] including heavy fermions[4] and dense quark matter.[5]

Recent progress of the preparation and manipulation of ultracold Fermi gases provides an ideal experimental platform of quantum simulation, which features a super clear system with unprecedented controllability, such that the single particle properties, the external environment and the inter-atom coupling can be tuned to a large extent. Thus, motivated by the first realization of pairing states in resonantly interacting alkali atoms with population imbalance,[6,7] a tremendous amount of effort has been devoted to the search of FFLO states in these systems. Many theoretical studies focused on the stable region of FFLO state in a uniform Fermi gas, and gave different conclusions by using various methods and approximations. In particular, some works claimed a fairly wide range of interaction covering both the weakly interacting Bardeen–Cooper–Schrieffer (BCS) regime and the Bose–Einstein condensate (BEC) regime for a stable FFLO phase,[8–10] while some others concluded a much narrower regime restricted within the BCS side of a narrow[11] and a wide[12] Feshbach resonances. Further studies also took realistic experimental conditions of finite temperature and harmonic trapping potential under consideration, and found that a stable FFLO state can only exist in a small region of a trap and at low temperatures with weak interaction.[13] With the consideration of these strict conditions, an unambiguous evidence for FFLO state is still lacking in polarized Fermi gases trapped in harmonic traps.

Another route towards the observation of FFLO state in ultracold Fermi gases is to implement an optical lattice. The presence of a lattice potential can assist the stabilization of FFLO states owing to two aspects. Firstly, the band structure generated by the lattice can feature von Hove singularities at an appropriate filling, leading to a nesting effect with significantly enhanced density of states to assist pairing.[14–16] Besides, the optical lattice can also provide an environment of reduced dimensionality, where a wider stable FFLO region is suggested.[17–24] Under this consideration, various methods have been proposed for detecting the FFLO state in optical lattices.[25–28] However, the FFLO state has so far eluded definite observation in ultracold atomic gases.

In this paper, we propose a scheme to stabilize the FFLO state in a two-component Fermi gas with equal population. We consider a two-dimensional (2D) Fermi gas trapped in a moving square optical lattice. In the frame moving with the lattice, the Cooper pairs acquire a finite external pair momentum, and

*Project supported by the Beijing Natural Science Foundation, China (Grant No. Z180013), the National Natural Science Foundation of China (Grant Nos. 11522436, 11774425, and 12074428), the National Key R&D Program of China (Grant No. 2018YFA0306501), and the Research Funds of Renmin University of China (Grant Nos. 16XNLQ03 and 18XNLQ15).

†Corresponding author. E-mail: kgao@ruc.edu.cn
‡Corresponding author. E-mail: wlzhang@ruc.edu.cn

© 2021 Chinese Physical Society and IOP Publishing Ltd

the superconducting state becomes unstable towards the normal state at a critical velocity. For systems around half filling, the underlying Fermi surface has nesting effect, such that the critical velocity acquires significant anisotropy and reaches its maximum when the velocity is parallel to the nesting vectors. When the external velocity is tilted from this optimal direction, we find that a spontaneous pair momentum of $\boldsymbol{q}_{\rm s}$ can be generated to take advantage of the nesting effect, leading to a possibility of a stable FFLO state in this equally polarized Fermi system.[29]

The remainder of this manuscript is organized as follows: In Section 2, we consider an equally populated two-component Fermi gas in a uniform two-dimensional square lattice, and present the formalism to derive the thermodynamic potential. By comparing the thermodynamic potential of the normal state and the super conducting state, we discuss the critical velocity of the system in Section 3. Specifically, we find that around half-filling where the system acquires nesting effect, the critical velocity is significantly enhanced when the lattice is moving along the nesting vector. In Section 4, we discuss the case where the lattice velocity is tilted away from the nesting vector, and show that the nesting effect can also be remarkable as it may spontaneously generate a pair momentum and lead to an FFLO state. We also map out the phase diagram of the system, and show the parameter region where the FFLO phase is stable against BCS and normal states. The main conclusions are summarized in Section 5.

2. Formalism

We first consider an equally populated Fermi gas confined in a static optical lattice and a quasi-two-dimensional trap, as described by the Hamiltonian (with natural units $\hbar = m = 1$)

$$\begin{aligned}\mathcal{H} = & \sum_{\sigma=\uparrow,\downarrow}\int \mathrm{d}^3\boldsymbol{r}\Psi_\sigma^\dagger(\boldsymbol{r})\left[-\frac{\nabla^2}{2}+V_{\rm ol}(\boldsymbol{r})+V_{\rm ext}(\boldsymbol{r})\right]\Psi_\sigma(\boldsymbol{r})\\ & +4\pi a_{\rm s}\int \mathrm{d}^3\boldsymbol{r}\Psi_\uparrow^\dagger(\boldsymbol{r})\Psi_\downarrow^\dagger(\boldsymbol{r})\Psi_\downarrow(\boldsymbol{r})\Psi_\uparrow(\boldsymbol{r}),\end{aligned} \tag{1}$$

where Ψ_σ ($\Psi_\sigma^\dagger$) represents the annihilation (creation) operator for fermion with spin σ, $V_{\rm ol}(\boldsymbol{r})$ and $V_{\rm ext}(\boldsymbol{r})$ are the optical lattice and global harmonic trapping potentials, respectively. With the natural units, in the following discussion we will use the symbol of wave vector to denote momentum and velocity. Here, we consider the case where fermions with opposite spins interact via a short-range s-wave interaction, which is characterized by the s-wave scattering length $a_{\rm s}$. The optical lattice potential takes the form $V_{\rm ol}(\boldsymbol{r}) = -[V_{0x}\sin^2(kx)+V_{0y}\sin^2(ky)+V_{0z}\sin^2(kz)]$, where V_{0x}, V_{0y}, and V_{0z} are the maximum depths of the external potential along corresponding directions, and $k = 2\pi/\lambda$ with λ the laser wavelength of the optical lattice.

Assuming the optical lattice is strongly confined in the z-direction, the atoms are localized within a single layer and all the excited degrees of freedom along the z-direction are frozen out. Then, this system can be described by a 2D Fermi–Hubbard model

$$\begin{aligned}\mathcal{H}-\mu N = & -\left(t_x\sum_{\langle \boldsymbol{i},\boldsymbol{j}\rangle_x}+t_y\sum_{\langle \boldsymbol{i},\boldsymbol{j}\rangle_y}\right)\left(\hat{c}_{\uparrow\boldsymbol{j}}^\dagger\hat{c}_{\uparrow\boldsymbol{i}}+\hat{c}_{\downarrow\boldsymbol{j}}^\dagger\hat{c}_{\downarrow\boldsymbol{i}}\right)\\ & +U\sum_{\boldsymbol{i}}\hat{c}_{\uparrow\boldsymbol{i}}^\dagger\hat{c}_{\downarrow\boldsymbol{i}}^\dagger\hat{c}_{\downarrow\boldsymbol{i}}\hat{c}_{\uparrow\boldsymbol{i}}-\mu\sum_{\boldsymbol{i},\sigma=\uparrow,\downarrow}\hat{c}_{\sigma\boldsymbol{i}}^\dagger\hat{c}_{\sigma\boldsymbol{i}}.\end{aligned} \tag{2}$$

Here, $\hat{c}_{\sigma\boldsymbol{i}}$ and $\hat{c}_{\sigma\boldsymbol{i}}^\dagger$ correspond to the fermionic annihilation and creation operators of atoms on the $\boldsymbol{i}$-th lattice site with spin σ, respectively, and $\langle \boldsymbol{i},\boldsymbol{j}\rangle_x$ denotes nearest neighbors in the x-direction. In principle, the parameter t and U can be computed numerically using the Wannier functions of the lowest band. Alternatively, we can also employ a harmonic approximation and obtain the following analytical expressions:

$$\frac{U}{E_{\rm R}} = 2^{\frac{5}{2}}\pi^{\frac{1}{2}}\frac{a_{\rm s}}{\lambda}(s_xs_ys_z)^{\frac{1}{4}}, \tag{3}$$

$$\frac{t_i}{E_{\rm R}} = \mathrm{e}^{-\pi^2\sqrt{s_i}/4}\left[\left(\frac{\pi^2 s_i}{4}-\frac{\sqrt{s_i}}{2}\right)-\frac{s_i}{2}(1+\mathrm{e}^{-\sqrt{s_i}})\right], \tag{4}$$

where $a_{\rm s}$ is the s-wave scattering length between two spin components, $E_{\rm R} = (2\pi/\lambda)^2/2$ is the recoil energy with λ the laser wavelength, and $s_i = V_{0i}/E_{\rm R}$ ($i = x,y,z$) labels the dimensionless height of the lattice potential. In the following discussion, we consider a 2D square lattice with $t_x = t_y = t$ and $\lambda = 1064$ nm, which is realized as a layer within an anisotropic quasi-2D optical lattice with $s_x = s_y = 2$ and $s_z = 10$. We set the scattering length $a_{\rm s} = -151.25a_{\rm B} = -8.004$ nm with $a_{\rm B}$ the Born radius, which corresponds to the case of $U/t = -4.1649$ and can be easily realized in experiment near a broad Feshbach resonance.

The Fermi–Hubbard model Eq. (2) cannot be solved exactly in the sense of thermodynamic limit. By adopting the mean-field approximation, the interacting term can be written as

$$\begin{aligned}\hat{c}_{\uparrow\boldsymbol{i}}^\dagger\hat{c}_{\downarrow\boldsymbol{i}}^\dagger\hat{c}_{\downarrow\boldsymbol{i}}\hat{c}_{\uparrow\boldsymbol{i}} = & \langle\hat{c}_{\uparrow\boldsymbol{i}}^\dagger\hat{c}_{\downarrow\boldsymbol{i}}^\dagger\rangle\hat{c}_{\downarrow\boldsymbol{i}}\hat{c}_{\uparrow\boldsymbol{i}}+\hat{c}_{\uparrow\boldsymbol{i}}^\dagger\hat{c}_{\downarrow\boldsymbol{i}}^\dagger\langle\hat{c}_{\downarrow\boldsymbol{i}}\hat{c}_{\uparrow\boldsymbol{i}}\rangle\\ & -\langle\hat{c}_{\uparrow\boldsymbol{i}}^\dagger\hat{c}_{\downarrow\boldsymbol{i}}^\dagger\rangle\langle\hat{c}_{\downarrow\boldsymbol{i}}\hat{c}_{\uparrow\boldsymbol{i}}\rangle.\end{aligned} \tag{5}$$

In the BCS theory, one can define an order parameter $\Delta \equiv U\langle\hat{c}_{\downarrow\boldsymbol{i}}\hat{c}_{\uparrow\boldsymbol{i}}\rangle$. Such a definition can be generalized to the FFLO state as $U\langle\hat{c}_{\downarrow\boldsymbol{i}}\hat{c}_{\uparrow\boldsymbol{i}}\rangle = \Delta\,\mathrm{e}^{2\mathrm{i}\boldsymbol{q}\cdot\boldsymbol{i}}$. For $\boldsymbol{q} = 0$, it gives the standard BCS solution, and for $\Delta = 0$, it gives the normal state. Using such an ansatz for the FFLO pairing, the Hamiltonian in momentum space can be written as

$$\begin{aligned}\mathcal{H}-\mu N = & \sum_{\boldsymbol{k}}\Big[\xi_{\boldsymbol{k}}(\hat{c}_{\uparrow\boldsymbol{k}}^\dagger\hat{c}_{\uparrow\boldsymbol{k}}+\hat{c}_{\downarrow-\boldsymbol{k}}^\dagger\hat{c}_{\downarrow-\boldsymbol{k}})\\ & +\Delta\hat{c}_{\uparrow\boldsymbol{q}+\boldsymbol{k}}^\dagger\hat{c}_{\downarrow\boldsymbol{q}-\boldsymbol{k}}^\dagger+\mathrm{h.c.}-\frac{|\Delta|^2}{U}\Big],\end{aligned} \tag{6}$$

where $\xi_{\boldsymbol{k}} = \varepsilon_{\boldsymbol{k}} - \mu$ is the single particle dispersion shifted by the chemical potential μ, and h.c. denotes Hermitian conjugate. The summation respected to $\boldsymbol{k}$ is restricted to the first Brillouin zone. In a 2D square lattice, the dispersion reads

$$\varepsilon_{\boldsymbol{k}} = 4\,t - 2\,t\,(\cos(k_x d) + \cos(k_y d))\,, \tag{7}$$

where $d = \lambda/2$ is the lattice spacing. Considering the fermionic anticommutator $\hat{c}^{\dagger}\hat{c} + \hat{c}\hat{c}^{\dagger} = 1$ and $\sum_{\boldsymbol{k}} \hat{c}^{\dagger}_{\uparrow \boldsymbol{k}} \hat{c}_{\uparrow \boldsymbol{k}} = \sum_{\boldsymbol{k}+\boldsymbol{q}} \hat{c}^{\dagger}_{\uparrow \boldsymbol{k}+\boldsymbol{q}} \hat{c}_{\uparrow \boldsymbol{k}+\boldsymbol{q}}$, the Hamiltonian can be rearranged in the matrix form

$$\begin{aligned}\mathcal{H} - \mu N = &\sum_{\boldsymbol{k}} \begin{pmatrix} \hat{c}^{\dagger}_{\uparrow \boldsymbol{k}+\boldsymbol{q}} & \hat{c}_{\downarrow -\boldsymbol{k}+\boldsymbol{q}} \end{pmatrix} \begin{pmatrix} \xi_{\boldsymbol{k}+\boldsymbol{q}} & \Delta \\ \Delta^* & -\xi_{-\boldsymbol{k}+\boldsymbol{q}} \end{pmatrix} \begin{pmatrix} \hat{c}_{\uparrow \boldsymbol{k}+\boldsymbol{q}} \\ \hat{c}^{\dagger}_{\downarrow -\boldsymbol{k}+\boldsymbol{q}} \end{pmatrix} \\ &+ \sum_{\boldsymbol{k}} \left(\xi_{-\boldsymbol{k}+\boldsymbol{q}} - \frac{|\Delta|^2}{U} \right). \end{aligned} \tag{8}$$

The matrix is then diagonalized to give the quasiparticle eigenenergies

$$E_{\boldsymbol{k},\boldsymbol{q},\pm} = \frac{\xi_{\boldsymbol{k}+\boldsymbol{q}} - \xi_{-\boldsymbol{k}+\boldsymbol{q}}}{2} \pm \sqrt{\xi_{\boldsymbol{q}}^2 + \Delta^2}, \tag{9}$$

where $\xi_{\boldsymbol{q}} = (\xi_{\boldsymbol{k}+\boldsymbol{q}} + \xi_{-\boldsymbol{k}+\boldsymbol{q}})/2$, and $\Delta = \Delta^*$ is assumed to be real without loss of generality. In order to diagonalize the Hamiltonian , we introduce a group of new operators $\hat{\gamma}_{\sigma,\boldsymbol{k},\boldsymbol{q}}$ and $\hat{\gamma}^{\dagger}_{\sigma,\boldsymbol{k},\boldsymbol{q}}$, which can be viewed as the quasiparticle annihilation and creation operators, and the relation between these new operators and the composite fermionic operators reads

$$\begin{pmatrix} \hat{c}_{\uparrow \boldsymbol{k}+\boldsymbol{q}} \\ \hat{c}^{\dagger}_{\downarrow -\boldsymbol{k}+\boldsymbol{q}} \end{pmatrix} = \begin{pmatrix} u_{\boldsymbol{k},\boldsymbol{q}} & v_{\boldsymbol{k},\boldsymbol{q}} \\ v_{\boldsymbol{k},\boldsymbol{q}} & -u_{\boldsymbol{k},\boldsymbol{q}} \end{pmatrix} \begin{pmatrix} \hat{\gamma}_{\uparrow \boldsymbol{k},\boldsymbol{q}} \\ \hat{\gamma}^{\dagger}_{\downarrow -\boldsymbol{k},\boldsymbol{q}} \end{pmatrix}. \tag{10}$$

The definitions of the coefficients are

$$\begin{aligned} u^2_{\boldsymbol{k},\boldsymbol{q}} &= \frac{1}{2}\left(1 + \frac{\xi_{\boldsymbol{q}}}{\sqrt{\xi_{\boldsymbol{q}}^2 + \Delta^2}}\right), \\ v^2_{\boldsymbol{k},\boldsymbol{q}} &= \frac{1}{2}\left(1 - \frac{\xi_{\boldsymbol{q}}}{\sqrt{\xi_{\boldsymbol{q}}^2 + \Delta^2}}\right), \\ u_{\boldsymbol{k},\boldsymbol{q}} v_{\boldsymbol{k},\boldsymbol{q}} &= \frac{\Delta}{2\sqrt{\xi_{\boldsymbol{q}}^2 + \Delta^2}}. \end{aligned} \tag{11}$$

By using these quasiparticle operators, the diagonalized Hamiltonian can be written as

$$\begin{aligned}\mathcal{H} - \mu N = &\sum_{\boldsymbol{k}} \begin{pmatrix} \hat{\gamma}^{\dagger}_{\uparrow,\boldsymbol{k},\boldsymbol{q}} & \hat{\gamma}_{\downarrow,-\boldsymbol{k},\boldsymbol{q}} \end{pmatrix} \begin{pmatrix} E_{\boldsymbol{k},\boldsymbol{q},+} & 0 \\ 0 & E_{\boldsymbol{k},\boldsymbol{q},-} \end{pmatrix} \begin{pmatrix} \hat{\gamma}_{\uparrow \boldsymbol{k},\boldsymbol{q}} \\ \hat{\gamma}^{\dagger}_{\downarrow -\boldsymbol{k},\boldsymbol{q}} \end{pmatrix} \\ &+ \sum_{\boldsymbol{k}} \left(\xi_{-\boldsymbol{k}+\boldsymbol{q}} - \frac{\Delta^2}{U} \right). \end{aligned} \tag{12}$$

We consider a grand canonical ensemble and the characteristic function is the grand potential $\Omega = -\frac{1}{\beta} \ln Z_{\mathrm{G}}$, where $Z_{\mathrm{G}} = \mathrm{Tr}\exp(-\beta(\mathcal{H} - \mu N))$ is the grand partition function. Considering the statistic property of the quasiparticles (i.e., $\hat{\gamma}^{\dagger}\hat{\gamma} = 0$ or 1), the partition function can be written as

$$Z_{\mathrm{G}} = \prod_{\boldsymbol{k}} \left(1 + \mathrm{e}^{-\beta E_{\boldsymbol{k},\boldsymbol{q},+}}\right) \left(1 + \mathrm{e}^{\beta E_{\boldsymbol{k},\boldsymbol{q},-}}\right) \mathrm{e}^{-\beta C}, \tag{13}$$

where $C = \xi_{-\boldsymbol{k}+\boldsymbol{q}} + E_{\boldsymbol{k},\boldsymbol{q},-} - \Delta^2/U)$ and $\beta = 1/(k_{\mathrm{B}}T)$. The thermodynamic potential then takes the form

$$\begin{aligned}\Omega = &\sum_{\boldsymbol{k}} \left[\xi_{-\boldsymbol{k}+\boldsymbol{q}} + E_{\boldsymbol{k},\boldsymbol{q},-} - \frac{\Delta^2}{U} \right] \\ &- \frac{1}{\beta} \sum_{\boldsymbol{k}} \ln \left(1 + \mathrm{e}^{-\beta E_{\boldsymbol{k},\boldsymbol{q},+}}\right) \left(1 + \mathrm{e}^{\beta E_{\boldsymbol{k},\boldsymbol{q},-}}\right), \end{aligned} \tag{14}$$

and can be reduced to the following expression at zero temperature

$$\begin{aligned}\Omega = &\sum_{\boldsymbol{k}} \Big[\xi_{-\boldsymbol{k}+\boldsymbol{q}} + E_{\boldsymbol{k},\boldsymbol{q},-} - \frac{\Delta^2}{U} \\ &+ E_{\boldsymbol{k},\boldsymbol{q},+}\Theta(-E_{\boldsymbol{k},\boldsymbol{q},+}) - E_{\boldsymbol{k},\boldsymbol{q},-}\Theta(E_{\boldsymbol{k},\boldsymbol{q},-}) \Big] \end{aligned} \tag{15}$$

with $\Theta(x)$ the Heaviside step function.

The thermodynamic potential is apparently a function of three parameters, i.e., the order parameter Δ, the pair momentum $\boldsymbol{q}$, and the chemical potential μ. For a given filling factor $n = N/M$ with M the total number of lattice sites, the equilibrium state can be obtained by minimizing Ω as a function of Δ and $\boldsymbol{q}$, while the chemical potential is determined self-consistently via the number equation

$$n = \frac{1}{M} \sum_{\boldsymbol{k}} \left(f(E_{\boldsymbol{k},\boldsymbol{q},+}) - f(E_{\boldsymbol{k},\boldsymbol{q},-})\right) \frac{\xi_{\boldsymbol{q}}}{\sqrt{\xi_{\boldsymbol{q}}^2 + \Delta^2}} + 1, \tag{16}$$

where $f(x) = 1/(\mathrm{e}^{\beta x} + 1)$ is the Fermi function. The solution with $\Delta = 0$ is by definition the normal state, while the one with finite order parameter is the pairing superfluid state. The latter category can be further distinguished as the BCS or FFLO state, which corresponds to a zero or finite pair momentum $\boldsymbol{q}$. We stress that the mean-field approach outlined above is commonly used to study the pairing physics in Fermi gases in traps or optical lattices.[13,15] Such a treatment can give a qualitative understanding about the stability of different pairing states in optical lattices, provided that the center-of-mass momentum remains small and higher band effect is not significant.

Next, we extend the discussion to a moving optical lattice with velocity $\boldsymbol{q}_{\ell}$. A moving optical lattice can be realized by inducing a small frequency detuning between the lasers forming the lattice, and has been successfully implemented with an acousto-optical modulator driven by phase-locked frequency generators.[30,31] Owing to the Galilean invariance, such a setup is equivalent to a superfluid with center-of-mass momentum $-\boldsymbol{q}_{\ell}$ flowing in the lattice frame. Thus, we can still use the formalism above to obtain the thermodynamic potential as Eq. (15). However, one should bear in mind that a BCS state

can not be considered in any sense as an FFLO state by such a frame transformation, as the center-of-mass velocity of the superfluid is imposed externally from the single-particle dispersion. An authentic FFLO state, on the other hand, is a result of interaction effect and should be spontaneously emerged.

3. Anisotropic critical velocity

The fact that the Fermi surface can be shifted by a particular vector to nest with another part of the Fermi surface is called Fermi surface nesting effect, and the particular vector is called the nesting vector, which is $(\pm\pi/d, \pm\pi/d)$ for a 2D square lattice. Nesting effect can significantly alter the thermodynamic properties of the system when the lattice is filled properly. On one hand, the density of states of a 2D square lattice would acquire a divergence at half filling (i.e., $n = 1$), such that the pairing instability can be drastically enhanced. On the other hand, when the optical lattice is moving at a given velocity, it is also natural to expect a lower energy if the velocity is parallel to the nesting vector than any other directions. As a consequence, the critical velocity of the superfluid state would be anisotropic owing to the anisotropy of the Fermi surface.

To show the anisotropy of critical velocity, we plot in Fig. 1 the amplitude of the critical velocity $q_c = |\boldsymbol{q}_c|$ for an optical lattice moving along different directions with filling factor $n = 0.9, 1.0$, and 1.1. The critical velocity is determined by comparing the thermodynamical potential between the pairing state with a finite order parameter and a normal state with $\Delta = 0$. For all filling factors, the critical velocity increases drastically as θ changes from zero to $\pi/4$. Here, θ is defined as the angle between the moving direction and one of the lattice principal axis, say the x direction. Thus, when $\theta \to \pi/4$, the moving velocity is aligned with the nesting vector, and the critical velocity diverges owing to the diverging density of states. One can also notice that the results of $n = 0.9$ and $n = 1.1$ are exactly identical as required by the particle–hole symmetry, and are always below the $n = 1.0$ case of a perfect nesting. To further analyze the effect of filling factor, we show in Fig. 2 the critical velocity as a function of n for two different moving directions. Notice that the line of $\theta = 0.156$ is always higher than the one of $\theta = 0.0$, and both curves reach their corresponding maximum at half filling $n = 1$.

These results clearly suggest that when the system is moving along the nesting vector of $\theta = \pi/4$, the superfluid state would benefit more from the enhancement of density of states, and can survive at a higher velocity. Since the moving velocity is equivalent to the center-of-mass velocity of the pairing order parameter, one would expect that an FFLO state can be favored if the pair momentum is tilted along the nesting vector. More interestingly, if an external movement of velocity q_x is applied to the lattice along the x-direction, it is possible to have a spontaneously generated wave vector q_y along the perpendicular direction, which tilts the original q_x towards the nesting vector to reduce energy. The system is then stabilized at an FFLO state which features a modulating order parameter along the y-direction. Naively, one may expect that when the induced wave vector is equal to the external one, i.e., $q_x = q_y$, the overall momentum becomes parallel to the nesting vector, and the pairing state would be optimally favored. However, this scenario also has a maximal amplitude of the overall q, which is detrimental to the survival of superfluidity. As a consequence, the true ground state of the system is determined by the competition between the nesting effect and the velocity induced energy increase.

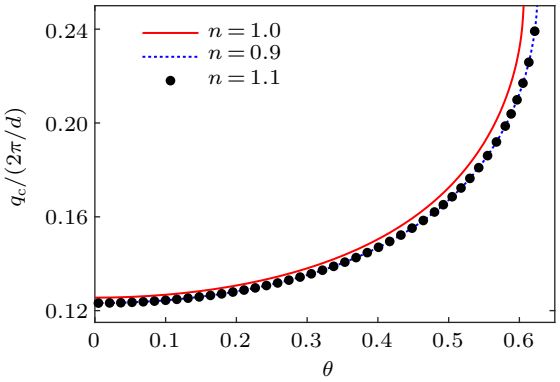


Fig. 1. The critical velocity at different moving directions. For filling factors $n = 0.9$, 1.0, and 1.1, q_c increases monotonically with increasing θ. When the lattice is moving along the nesting vector with $\theta = \pi/4$, the critical velocity becomes divergent. The results for $n = 0.9$ and 1.1 are identical as required by the particle-hole symmetry of this system.

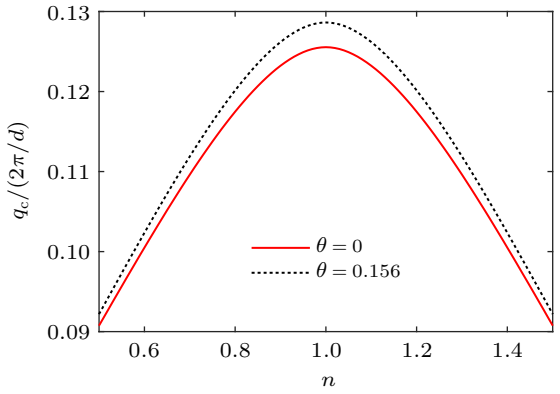


Fig. 2. The critical velocity of different moving directions with respect to the filling factor. Notice that the anisotropy of q_c reaches its maximum at half filling $n = 1.0$, at which a perfect nesting is reached.

4. FFLO states induced by moving lattice

To investigate the existence and property of the FFLO state as mentioned above, in this section we calculate the zero temperature thermodynamic potential Ω of the system, when subjected to an external velocity q_x and a spontaneously generated modulation q_y. In Fig. 3, we show the contour plots of thermodynamic potential for different choices of q_x by varying the order parameter Δ and q_y, where the filling factor is fixed at $n = 1$ by solving the number equation (16) self-consistently. The value of Ω for different panels are shifted to zero at their

corresponding ground state, such that a clear comparison can be made.

When the external velocity q_x is small, there is only one minimum of the thermodynamic potential with a finite order parameter Δ and $q_y = 0$ as shown in Fig. 3(a), indicating a conventional BCS state. As increasing q_x beyond a certain value, another minimum starts to appear at $\Delta \neq 0$ and $q_y \neq 0$. However, this FFLO state is only metastable as depicted in Fig. 3(b), and the true ground state of the system is still the BCS state. When q_x is further elevated, the difference between the FFLO and BCS state is reduced, and finally the two states become energetically degenerate. A first order phase transition would take place at this critical point as shown in Fig. 3(c). Notice that the value of $q_y \approx 0.6134 q_x$ at the phase transition point, which corresponds to an angle of $\theta \approx 0.55$, and is significantly deviated from the nesting vector with $q_y = q_x$ and $\theta = \pi/4$. Beyond this transition point, the FFLO state remains as the global minimum with even larger q_x, as depicted in Fig. 3(d).

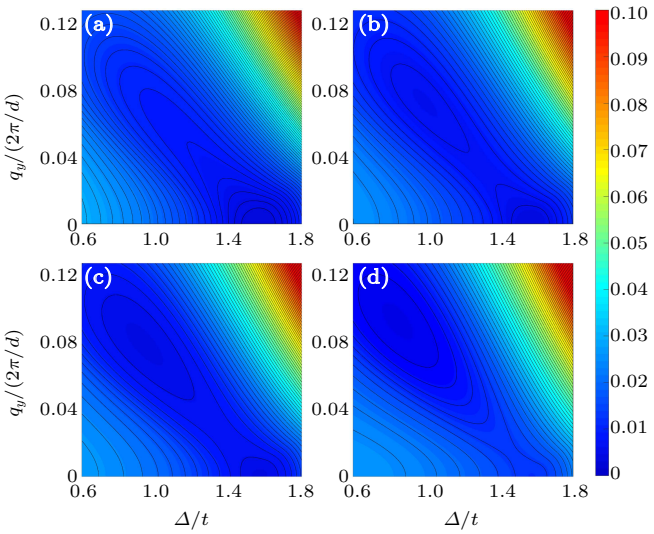


Fig. 3. The false color plots of zero temperature thermodynamic potential Ω by varying the order parameter magnitude Δ and pair momentum along the y direction q_y. In this figure, the filling factor is $n = 1.0$, and the external velocity is (a) $q_x = 0.126$, (b) $q_x = 0.130$, (c) $q_x = 0.13189$ and (d) $q_x = 0.137$. In each panel, the value of Ω is shifted to be zero at the corresponding ground state.

According to the analysis above, it is clear that the phase transition between BCS and FFLO states is of first order, characterizing by a sudden change of the order parameter. In Fig. 4, we show the amplitude of order parameter at zero temperature with respect to the variation of the external velocity by fixing $n = 1.0$. It can be seen that when the external velocity is less than the critical value, i.e., $q_x \approx 0.13189$, the order parameter of the BCS phase almost has no response to the variation of q_x. However, by crossing the transition point, a sharp jump occurs which is a doubtless evidence of a first order phase transition. As we continue to increase the external velocity, the amplitude of the order parameter decreases, but does not tend to zero even when q_x reaches the boundary of the Brillouin zone. This implies that the system will not enter the normal phase, which is a natural expectation for a mean-field approach of a system with perfect nesting and diverging density of states.

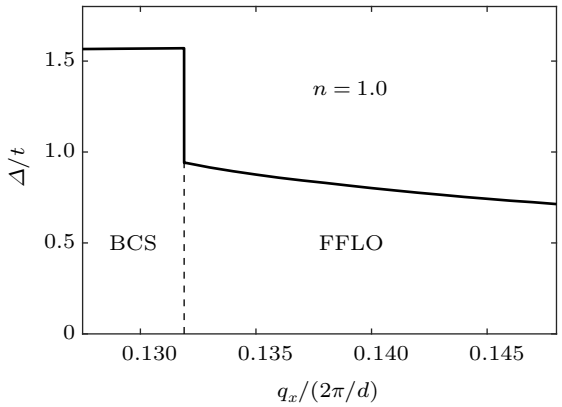


Fig. 4. The change of order parameter by crossing the first order transition from BCS to FFLO states, showing an abrupt change at the critical point (dashed line).

The first order transition between BCS and FFLO states can also be characterized by the direction of the pair momentum $\boldsymbol{q}$. As shown in Fig. 5, a local minimum of FFLO state starts to emerge at $q_x \approx 0.1276$ with a momentum tilting of $\theta \approx 0.4363$. By increasing the external velocity, the angle θ is also increased monotonically, but the FFLO state remains metastable until the first order transition point is reached. Beyond the phase transition, θ also increases with q_x, indicating that the system tends to take advantage of the perfect nesting effect at $\theta = \pi/4$. This result implies that although a modulation of the order parameter along the y-axis tends to enhance the magnitude of the overall wave vector $\boldsymbol{q}$ and is usually considered to be detrimental to the superfluid state, in the present case the nesting effect will become more crucial with increasing q_x.

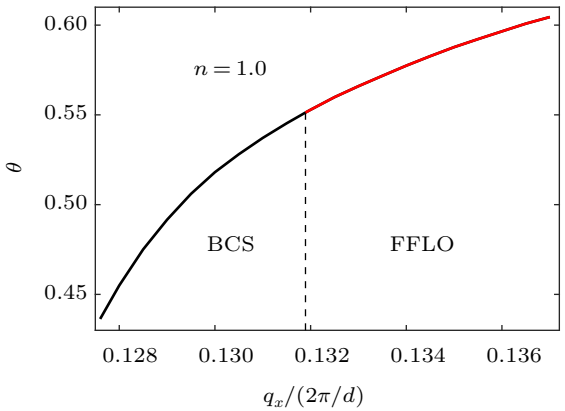


Fig. 5. The change of the direction of pairing order parameter with respect to the external velocity. With increasing q_x, a metastable FFLO state with a finite θ (black solid line) starts to appear at $q_x \approx 0.1276$, which becomes the true ground state (red solid line) beyond the critical point (dashed line).

With the understanding of the emergence FFLO state at $n = 1.0$, we generalize the discussion to other filling factors. In Fig. 6, we show the phase diagram of the system by varying the

external driving velocity q_x and the filling factor $0.2 < n < 1.8$. Apparently, the phase diagram is symmetric with respect to half filling as required by the particle-hole symmetry. On this phase diagram, the ground state of each parameter choice is determined by minimizing the thermodynamic potential as in Fig. 3 to avoid the possibility of finding a local minimum or saddle point when solve the gap and number equations.

When the filling factor n is less than 0.59 (or symmetrically higher than 1.41), a first order phase transition would take place from the BCS state to the normal phase as q_x increasing. By crossing the transition point, the order parameter features a sudden change, leading to a discontinuous behavior in many thermodynamic properties. As a result, a phase separation regime exists between the BCS and normal states to minimize the free energy in the canonical ensemble. When the filling factor n moves towards half filling with $0.59 \lesssim n \lesssim 0.82$ (or symmetrically $1.18 \lesssim n \lesssim 1.41$), an FFLO phase can be stabilized as increasing q_x from the BCS state, and eventually gives its way to the normal phase with even higher q_x. While the BCS–FFLO transition is also of the first order with a phase separation region between the BCS and FFLO states, the transition from the FFLO to the normal phase is of the second order. For filling factor even closer to half filling, $0.82 \lesssim n \lesssim 1.18$, the FFLO state can persist until q_x reaches the boundary of the Brillouin zone, owing to the significant enhancement of density of states induced by the nesting effect. From this phase diagram, we can clearly notice that the FFLO phase only exists when the filling factor is around half filling. This observation gives a further evidence that such an exotic pairing state crucially relies on the nesting of Fermi surface, which is significant only near half filling.

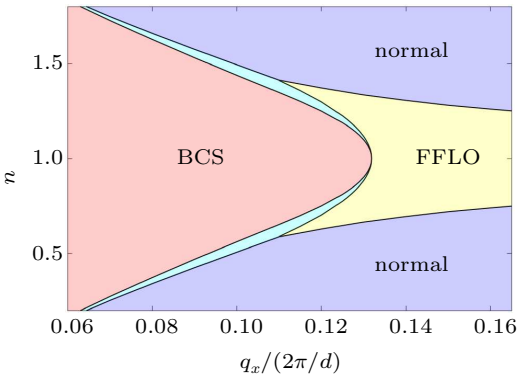


Fig. 6. The phase diagram of the system at zero temperature. By varying the filling factor and external velocity, four different phases can be located by minimizing the thermodynamic potential, including the BCS state (pink), the FFLO state (yellow), the normal phase (light blue), and a narrow region of phase separation (cyan).

5. Conclusion

We consider a two-component Fermi gas loaded in a two-dimensional square optical lattice, which is dragged to move with a certain velocity q_x along one of the principal axis (e.g., x-axis). Within a mean field approach, we determine the ground state of such a system by minimizing the thermodynamic potential at zero temperature. We find that for a filling factor around half filling, an FFLO state with a finite center-of-mass paring momentum can be stabilized when the moving velocity q_x exceeds a critical value. This exotic pairing state is characterized by a spontaneously generated modulation with wave vector q_y along the perpendicular direction, such that the total pair momentum of the order parameter is tilted towards the nesting vector $\boldsymbol{Q} = (\pm\pi/d, \pm\pi/d)$. By doing so, the pairing state can be energetically favorable owing to the enhancement of density of states. We characterize the first order phase transition between the BCS and the FFLO states with increasing q_x, and map out the phase diagram for a wide range of filling factor. The stability region of the FFLO state may be even enlarged when considering a more general state with a combination of multiple pairing momenta, which is usually energetically more favorable than the single-component solution.

References

[1] Fulde P and Ferrel R A 1964 *Phys. Rev.* **135** A550
[2] Larkin A I and Ovchinnikov Y N 1965 *Sov. Phys. JETP* **20** 762
[3] Casalbuoni R and Nardulli G 2004 *Rev. Mod. Phys.* **76** 263
[4] Radovan H A, Fortune N A, Murphy T P, Hannahs S T, Palm E C, Tozer S W and Hall D 2003 *Nature* **425** 51
[5] Alford M, Bowers J A and Rajagopal K 2001 *Phys. Rev. D* **63** 074016
[6] Zwierlein M W, Schirotzek A, Schunck C H and Ketterle W 2006 *Science* **311** 492
[7] Partridge G B, Li W, Kamar R I, Liao Y and Hulet R G 2006 *Science* **311** 503
[8] Machida K, Mizushima T and Ichioka M 2006 *Phys. Rev. Lett.* **97** 120407
[9] Kinnunen J, Jensen L M and Törmä P 2006 *Phys. Rev. Lett.* **96** 110403
[10] He Y, Chien C C, Chen Q J and Levin K 2007 *Phys. Rev. A* **75** 021602(R)
[11] Sheehy D E and Radzihovsky L 2006 *Phys. Rev. Lett.* **96** 060401
[12] Yi W and Duan L M 2006 *Phys. Rev. A* **73** 031604(R)
[13] Zhang W and Duan L M 2007 *Phys. Rev. A* **76** 042710
[14] Koponen T K, Paananen T, Martikainen J P and Törmä P 2007 *Phys. Rev. Lett.* **99** 120403
[15] Koponen T K, Paananen T, Maitikainen J P, Bakhtiari M R and Törmä P 2008 *New J. Phys.* **10** 045014
[16] Cui X and Wang Y 2010 *Phys. Rev. A* **81** 023618
[17] Yang K 2001 *Phys. Rev. B* **63** 140511
[18] Orso G 2007 *Phys. Rev. Lett.* **98** 070402
[19] Hu H, Liu X J and Drummond P D 2007 *Phys. Rev. Lett.* **98** 070403
[20] Feiguin A E and Heidrich-Meisner F 2007 *Phys. Rev. B* **76** 220508
[21] Parish M M, Baur S K, Mueller E J and Huse D A 2007 *Phys. Rev. Lett.* **99** 250403
[22] Conduit G J, Conlon P H and Simons B D 2008 *Phys. Rev. A* **77** 053617
[23] Batrouni G G, Huntley M H, Rousseau V G and Scalettar R T 2008 *Phys. Rev. Lett.* **100** 116405
[24] Rizzi M, Polini M, Cazalilla M A, Bakhtiari M R, Tosi M P and Fazio R 2008 *Phys. Rev. B* **77** 245105
[25] Radzihovsky L and Sheehy D E 2010 *Rep. Prog. Phys.* **73** 076501
[26] Korolyuk A, Massel F and Törmä P 2010 *Phys. Rev. Lett.* **104** 236402
[27] Swanson M, Loh Y L and Trivedi N 2012 *New J. Phys.* **14** 033036
[28] Kajala J, Massel F and Törmä P 2011 *Phys. Rev. A* **84** 041601(R)
[29] Doh H, Song M and Kee H Y 2006 *Phys. Rev. Lett.* **97** 257001
[30] Fallani L, De Sarlo L, Lye J E, Modugno M, Saers R, Fort C and Inguscio M 2004 *Phys. Rev. Lett.* **93** 140406
[31] Mun J, Medley P, Campbell G K, Marcassa L G, Pritchard D E and Ketterle W 2007 *Phys. Rev. Lett.* **99** 150604